Journal of Environmental Management 301 (2022) 113791

Contents lists available at ScienceDirect

Journal of Environmental Management

journal homepage: www.elsevier.com/locate/jenvman

Conversion of pyrolytic non-condensable gases from polypropylene co-polymer into bamboo-type carbon nanotubes and high-quality oil using biochar as catalyst

Kalpit Shah [a,b,*], Savankumar Patel [a,b], Pobitra Halder [a,b], Sazal Kundu [a], Mojtaba Hedayati Marzbali [a], Ibrahim Gbolahan Hakeem [a], Biplob Kumar Pramanik [c], Ken Chiang [a], Tejas Patel [a]

[a] Chemical & Environmental Engineering, School of Engineering, RMIT University, Melbourne, Victoria, 3000, Australia
[b] ARC Training Centre for Transformation of Australia's Biosolids Resource, RMIT University, Bundoora, Victoria, 3083, Australia
[c] Civil and Infrastructure Engineering, School of Engineering, RMIT University, Melbourne, Victoria, 3000, Australia

ARTICLE INFO

Keywords:
Carbon nanotubes
Biochar catalyst
Chemical vapour deposition
Waste plastics
Waste management
Circular economy

ABSTRACT

The conversion of low-value plastic waste into high-value products such as carbon nanomaterial is of recent interest. In the current study, the non-condensable pyrolysis gases, produced from Polypropylene Copolymer (PPC) feedstock, was converted into bamboo-type carbon nanotubes (BCNTs) through catalytic chemical vapour deposition using biochar. Experiments were conducted in a three-zone furnace fixed bed reactor, where PPC was pyrolysed in the second zone and carbon nanotubes (CNTs) growth was eventuated in the third zone. The effects of different growth temperatures (500, 700, 900 °C) and biochar particle sizes (nanoparticle as well as 0–100 and 100–300 μm) were investigated to optimise the production of hydrogen and the yield of carbon nanotubes on the biochar surface. Biochar samples used in the synthesis of CNTs were obtained from the pyrolysis of saw dust at 700 °C in a muffle furnace. Analyses performed by using Scanning electron microscopy, Transmission electron microscopy, X-ray diffraction, and Raman spectroscopy techniques suggested that the best crystalline structure of CNTs were obtained at 900 °C with nano-sized biochar as a catalyst. The strong gas-solid contact and void fraction of nano-sized particles enhances the diffusion–precipitation mechanism, leading to the growth of CNTs. The nano-sized biochar increased hydrogen production at 900 °C and reduced the polycyclic aromatic hydrocarbons content in oil to only 1%, which is advantageous for further utilisation. Therefore, the production of high-value CNTs from waste plastic using low-cost biochar catalyst can be a sustainable approach in the management of waste plastic while participating in the circular economy.

1. Introduction

Most polymers are mass-manufactured and inexpensive, thereby they are discarded readily after being used. Recently, the methods of recycling and recovery of waste plastics are promoted instead of the existing widespread incineration and landfilling practices due to their high energy value. However, the rate of global recycling and recovery is still not very high, and it differs across various geographic areas (Zhuo and Levendis, 2014). In 2015, nearly 20% of global plastic waste was recycled, 25% was incinerated and 55% was landfilled (Ritchie and Roser, 2020). In addition, only 9% of plastic waste, generated between 1950 and 2015, was recycled (Ritchie and Roser, 2020). The properties of recycled plastics are often compromised and are not suitable for their original applications (Al-Salem et al., 2009). The recycled plastics are particularly used for packaging and other fast-moving consumer goods, where they participate in the circular economy by downcycling their original values. Apart from this, the recycled plastics should not be used in the medicine and food sectors. Therefore, recycling may not be an attractive solution in the world for circular economy. Bio-plastic, produced from bio-materials such as fruits and vegetables waste can be an environmentally sustainable and circular approach alternative to petroleum-based traditional plastics (Acquavia et al., 2021). However, only 1% of total global plastic generation (360 million tons) is being produced from bio-materials, which emphasises on the exploration of

* Corresponding author. Chemical & Environmental Engineering, School of Engineering, RMIT University, Melbourne, Victoria, 3000, Australia.
E-mail address: kalpit.shah@rmit.edu.au (K. Shah).

https://doi.org/10.1016/j.jenvman.2021.113791
Received 22 January 2021; Received in revised form 26 August 2021; Accepted 18 September 2021
Available online 27 September 2021

Table 1
Product yields and carbon produced from PPC.

Particle size	Temperature (°C)		Yield (%)		Carbon deposit on catalyst (g)	Carbon deposition rate ($mg.h^{-1}/g_{catalyst}$)
	Pyrolysis	CVD	Gas	Liquid		
100–300 μm	500	500	75.17 ± 1.11	24.83 ± 1.11	0.000 ± 0	0.0 ± 0
100–300 μm	500	700	77.12 ± 0.9	22.81 ± 0.91	0.007 ± 0.001	1.4 ± 0.2
100–300 μm	500	900	78.49 ± 0.75	21.02 ± 0.8	0.047 ± 0.003	9.4 ± 0.6
0–100 μm	500	500	75.16 ± 1.0	24.83 ± 1.0	0.001 ± 0	0.2 ± 0
0–100 μm	500	700	77.11 ± 0.8	22.81 ± 0.82	0.008 ± 0.001	1.6 ± 0.2
0–100 μm	500	900	78.44 ± 0.9	21.02 ± 0.97	0.051 ± 0.004	10.2 ± 0.8
Nano	500	500	75.13 ± 0.6	24.82 ± 0.61	0.005 ± 0.001	1.0 ± 0.2
Nano	500	700	77.07 ± 0.75	22.81 ± 0.78	0.011 ± 0.001	2.2 ± 0.2
Nano	500	900	78.15 ± 1.2	21.03 ± 1.31	0.078 ± 0.004	15.6 ± 0.8
No catalyst	500		75.15 ± 0.8	24.85 ± 0.8		

circular approach for plastic wastes management. Considering the current scenario of plastic wastes management, alternative circularities are in demand for plastic wastes and it is possible to produce high-value products such as carbon nanotubes (CNTs) and/or carbon nanofibers (CNFs) from this low-cost waste, which upcycles the waste material and maintains the environmental sustainability (Bazargan and McKay, 2012; Zhuo and Levendis, 2014). The upcycling of waste plastics into high-value CNTs rather than their traditional recycling can be an attractive route of circular economy that can improve the environmental sustainability.

CNTs can be used for many advanced applications in various sectors such as textile (Kang et al., 2010), ultra-strong fibres (Kang et al., 2010), hydrogen storage (Chen et al., 2010), electronics (Kalita et al., 2009), fuel cell (Jin et al., 2007), microwave absorption (Narayanan et al., 2009), manufacture of nano-cables and transistors (Lefebvre and Ding, 2017), catalysis process (Liu et al., 2018b; Louisia et al., 2018), actuator (Biso and Ricci, 2009), and biomedical (Zanello et al., 2006). So far, a number of methods have been developed for the synthesis of CNTs, for example, laser ablation (Guerrero et al., 2008), arc discharge (Berkmans et al., 2014), plasma-assisted deposition (Chhowalla et al., 2001), pyrolysis (Liu et al., 2003), and thermal chemical vapour deposition (CVD) (Reddy et al., 2006). Among these methods, the most widely used thermal CVD is a relatively low-cost technology, which can produce high-quality CNTs at a large scale (Paradise and Goswami, 2007; Song and Ji, 2011).

Methane or natural gas has been used as a major carbon precursor for the production of CNTs and hydrogen production using the CVD method (Ahmed et al., 2016; Awadallah et al., 2016). Various studies have attempted to use alternative sources of carbon including ethylene (Cheng, 2012; In et al., 2011; Savva et al., 2010), acetylene (Perez-Cabero et al., 2003; Qin et al., 2004), toluene, aromatic hydrocarbons, xylenes, benzene and alcohols (Das et al., 2006; Ren et al., 2014; Shaikjee and Coville, 2012; Shirazi et al., 2011). A more environmental and economical method for carbon nanomaterial (CNM) production is of great interest to industry. Cost-effective and innovative alternative sources such as plastic waste as a carbon source can be very attractive in this sense (Arena et al., 2006; Gong et al., 2014; Liu et al., 2011; Mishra et al., 2012). According to the literature, CNTs have been produced through either a one-stage process (Gong et al., 2012, 2013; Mishra et al., 2012) or a two-stage process (Aboul-Enein et al., 2017; Borsodi et al., 2016; Liu et al., 2011). In the one-stage process, precursor and catalyst are mixed together and therefore, temperature of pyrolysis and CVD cannot be controlled. However, in the two-stage process, temperature in each stage can be easily and independently controlled. Two-stage process enhances the interaction between the pyrolysis gases and catalyst compared to one-stage process. Most importantly, the deposited carbon and reacted catalysts can be easily recovered, recycled and reused in the two-stage process.

The pyrolysis vapours, produced from the pyrolysis of waste plastics, can be the main source for the formation of CNTs on the surface of catalyst. However, the yield and quality of CNTs depends on the temperature, type of plastic polymer, reaction time, catalyst, and reactor used in the CNT synthesis (Bazargan and McKay, 2012; Zhuo and Levendis, 2014). Aboul-Enein et al. (2018) demonstrated large gas yields from the pyrolysis of polypropylene (PP) and low-density polyethylene (LDPE) as well as the formation of high quality of CNTs with high yield over Ni–Mo/Al_2O_3 catalyst. However, the use of polystyrene (PS) or polyethylene terephthalate (PET) waste as carbon precursor provided a low yield and poor quality CNTs. Mishra et al. (2012) used a one-stage method to convert waste PP into Multi-Wall CNTs (MWCNTs) via chemical vapour deposition using nickel (Ni) catalyst. Liu et al. (2011) and Borsodi et al. (2016) used a two-stage reactor to convert PP into CNTs with HZSM-5 and Fe or Co as catalysts. Kong and Zhang (2007) and Zhang et al. (2008) demonstrated that PE and maleated polypropylene (MA-PP) can be used as precursors for the synthesis of CNTs, using ferrocene/Ni as catalyst at 700 °C for 100 min. Liu et al. (2011) used a screw kiln reactor for the production of hydrocarbon gases from catalytic pyrolysis of PP, which were used for the synthesis of CNTs. Zhuo et al. (2012) used a two-step process, a combination of pyrolysis and CVD methods, for the production CNTs from municipal plastic waste. Nahil et al. (2015) explored the use of a Ni-based catalyst to pyrolyse and reform heterogeneous mixed plastic waste into hydrogen and CNTs. Chung et al. (Chung and Jou, 2005) observed that the CNTs synthesised from the catalytic pyrolysis of PP were composed of wavy carbon layers.

Many studies suggest that the use of transition metals as catalysts can produce high yield and quality of CNTs (Aboul-Enein et al., 2018; Borsodi et al., 2016; Mishra et al., 2012). However, transition metal catalysts, amorphous carbon and CNTs need to be separated after the CVD process via chemical and/or thermal treatment which may not be cost-effective (Ghosh, 2018). Transition metal catalysts are highly toxic to health and environment. In addition, transition metal catalysts are costly and thereby, it is important to find a cost-effective process for CNTs synthesis. Biochar can be an effective carbo-catalyst for CVD process. Biochar can be produced from the pyrolysis of low-cost and readily available waste biomass materials, which can take part in the circular economy as well as environmental sustainability by properly managing the waste materials. However, the effectiveness of biochar as a catalyst for CVD process requires to be benchmarked with transition metal catalysts. Recently, efforts have been made for the production of CNTs from the pyrolysis of methane using metal-loaded biochar as a catalyst in a microwave-assisted process. Hildago-Oporto et al. (2019) synthesised CNTs from the pyrolysis of methane using hazelnut hull and wheat straw derived biochar and ferrocene loaded biochar catalyst. The biochar was produced at 600 °C using microwave irradiation. The researchers observed a higher degree of CNTs wall graphitisation with a smaller hydrodynamic diameter. Zhang et al. (2019) also obtained tubular and multiwall CNTs using Ni-loaded biochar as catalyst.

To the best of our knowledge, there is no study on the application of biochar only as a catalyst produced from the pyrolysis of biomass to decompose non-condensable hydrocarbons produced from the pyrolysis of Polypropylene Copolymer (PPC) for the formation of CNTs. The

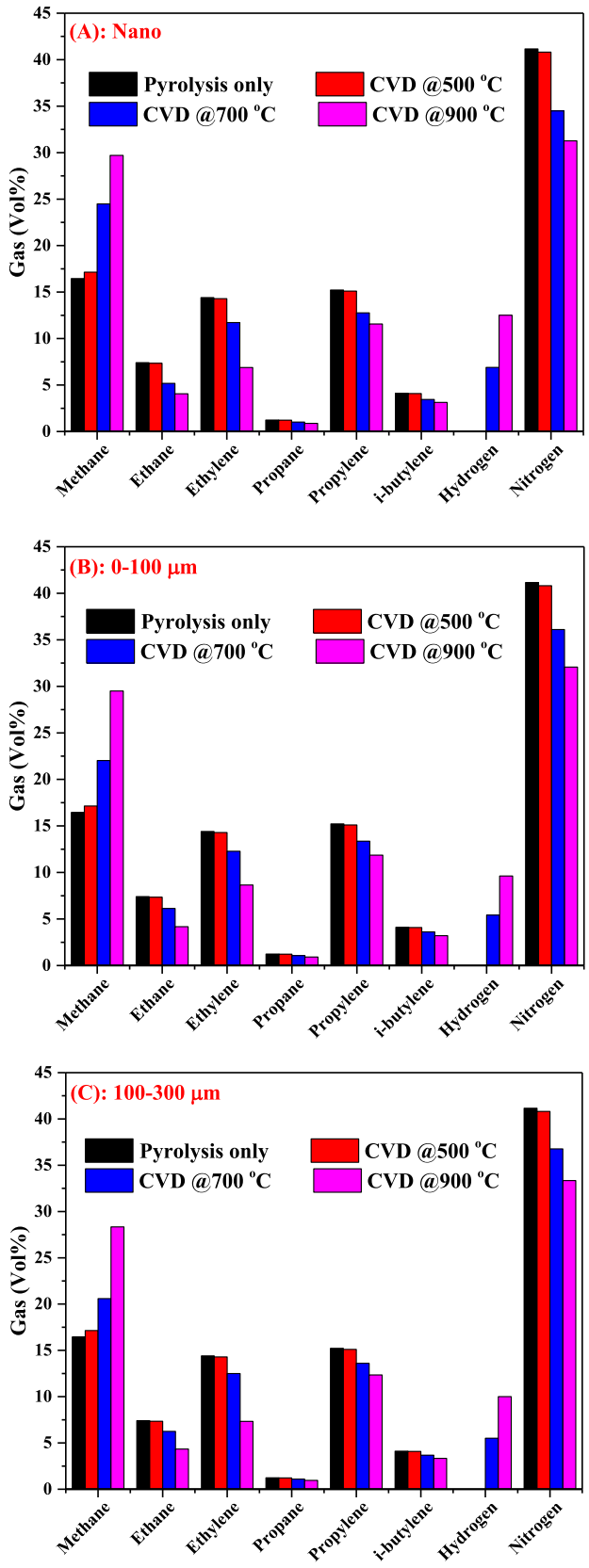

Fig. 1. Composition of the non-converted pyrolysis gas in the presence of biochar with different particle size (A) nano-sized particle, (B) 0–100 µm and (C) 100–300 µm.

specific objectives of the current work include (i) study the applicability of biomass-derived biochar as a catalyst to catalyse the carbonisation of PPC to form large quantities and high-quality CNTs, (ii) investigate the production of CNTs and its morphological behaviour at different CVD temperatures and the biochar particle sizes and (iii) study the effect of CVD temperatures and the biochar particle sizes on liquid oil product composition. Biochar, produced from the low-cost and readily available biomass, may have excellent physico-chemical properties such as functional groups, surface area and micro-pore volume, which may allow it to act as a carbon precursor, substrate and catalyst for enhancing CNT growth from hydrocarbon vapours, produced from the pyrolysis of waste plastics. In addition, at the same time, biochar may also act as a catalyst for thermal cracking of oil produced from waste plastics pyrolysis and improve its quality. Therefore, the current study will propose a new circular way of managing plastic wastes and producing high-value products using low-cost material.

2. Materials and methods

2.1. Experimental setup

The pyrolysis and CVD experiment for the formation of CNTs from PPC waste was performed using two-step process inside a long quartz tube reactor (ID = 27 mm and length = 1000 mm) as shown in Fig. S1. The experiment was performed for 1 h. An electrically heated furnace, comprised of three different heating zones, was used to provide thermal energy to the reactor. Waste PPC bottle, collected from laboratory, was used in the present work. The samples were washed, air-dried and shredded into small pieces between 50 and 600 µm. Precisely, 10 g of PPC sample was placed nearly in the middle of the reactor positioning the sample at the second zone of the furnace, where pyrolysis occurs. At the third zone of the furnace (or simply called the CVD zone), 5 g of the biochar catalyst was charged inside the reactor. Zone I was kept empty and used for pre-heating of inert gas (i.e. N_2) entering the reactor. Biochar catalyst was prepared from the pyrolysis of mixed sawdust, collected from RMIT University workshop, using a muffle furnace. The pyrolysis of biomass was carried out at 700 °C. The physical and chemical properties of PPC and biochar, used in the current study is presented in Table S1. The temperature of PPC pyrolysis in Zone II and hydrocarbon vapour decomposition in Zone III were controlled using two different electrical controllers. A controlled N_2 (100 mL/min) gas flow was used to provide an inert environment. The initial ramp rate of 35 °C/min was fixed for all experiments for the reactor to reach the operating temperature. The effect of CVD temperature (i.e., from 500 to 900 °C) and biochar particle size (i.e., from nano to micro size) were investigated in detail on the conversion of PPC into its vapour constituents, CNM production and morphological transformations. Throughout the study, plastic pyrolysis was conducted at 500 °C. Larger-sized particles such as 100–300 and 0–100 µm were obtained from the sieving of biochar that is produced from muffle furnace while nano-sized particles were prepared using the sonication bath as per the procedure described elsewhere (Liu et al., 2018a). Each experiment was replicated three times. The data presented in the manuscript, therefore, represent the average values of three experimental data obtained under the same condition.

2.2. Product analysis methods

The gases produced from the experiment were measured using an online micro-GC (Agilent, micro-GC 490) analyser. The gases were sampled every 4 min by micro-GC for the analysis. The micro-GC was calibrated using standard calibration gases. Then, the components of the pyrolysis gas were identified and the composition (vol%) of the gas was measured based on the calibration of standard gases. The produced carbon material (biochar and deposited carbon such as carbon nanotubes on the surface of biochar) was cooled to room temperature by

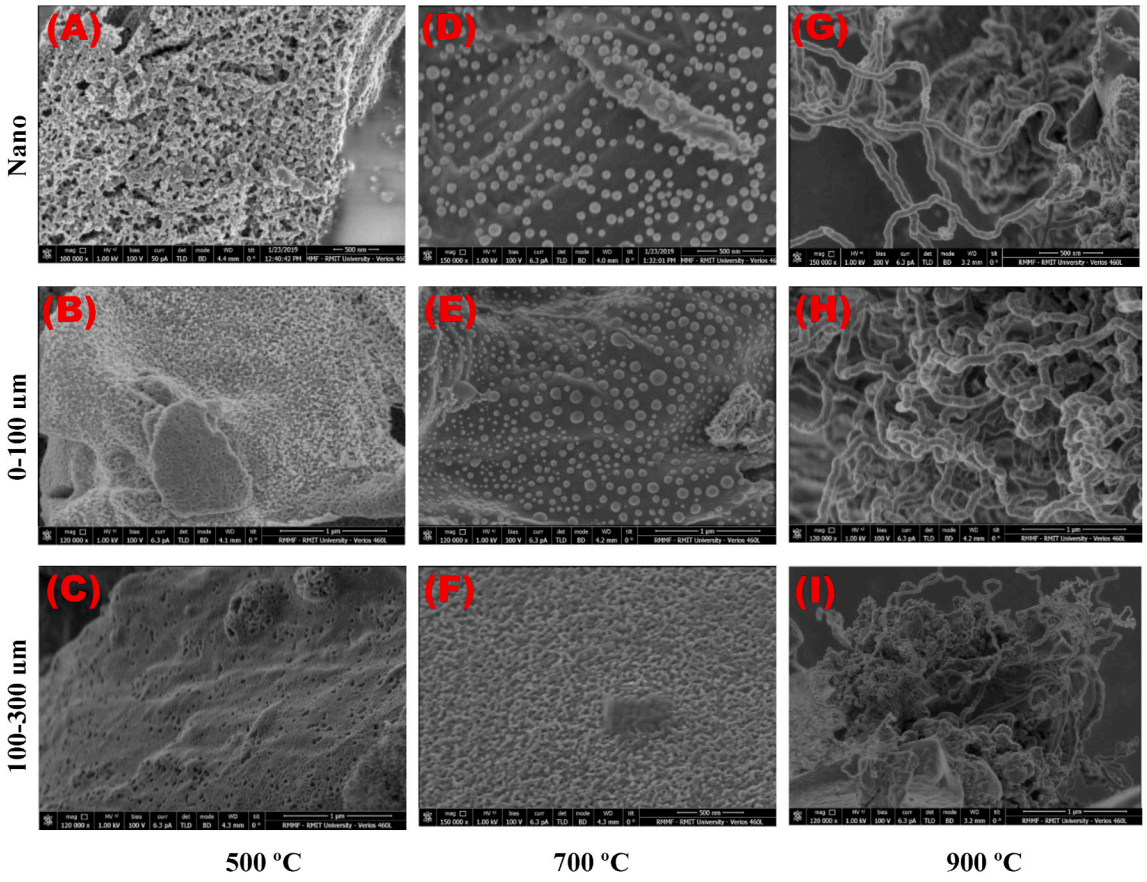

Fig. 2. SEM images of biochar samples with CNTs at different CVD temperatures and biochar particle size.

using 100 ml/min of N_2 as a cooling gas. Scanning electron microscopy (SEM) imaging of deposited carbon samples was performed using a FEI Verios 460L instrument. Transmission Electron Microscopy (TEM) analysis was carried out using a JEOL-1010 microscope. For TEM analysis, the samples were initially finely grounded, dispersed in isopropyl alcohol (IPA) and a drop of this solution was then introduced on a classical TEM carbon grid. XRD spectroscopic analysis was performed using a Bruker Axs D4 Endeavor Wide Angle X-Ray Diffraction instrument fitted with a copper tube (Cu Kα radiation). A PerkinElmer Raman Station 400F instrument was used for Raman spectroscopic analysis of carbon deposited on biochar samples. The pyrolysis oil, produced during the process, was analysed using a GC-MS (Agilent, GC-7890A, MS-5975C), equipped with a HP-5 capillary column (length = 30 m, ID = 0.25 mm and film thickness = 0.25 μm). The column temperature was set at 45 °C for 3 min and then increased to 250 °C at 7 °C/min. Finally, the column temperature was maintained at 250 °C for 5 min. The ion source temperature was also maintained at 250 °C. High purity helium gas was used as the carrier gas.

2.3. Modelling study

The process modelling was performed using ASPEN Plus software assuming steady-state conditions, zero-dimensional model, isothermal bed (uniform bed temperature). As can be seen from Fig. S2, the stream POLY-PRO was specified as a non-conventional stream and the ultimate and proximate analyses of PPC were used as the input. The thermodynamic conditions and mass flow rate of streams were entered as used in the experimental section. The PPC (POLY-PRO) enters in the pyrolysis yield reactor (Y-PYRO), where yields were set by a calculator block, which in turn determines the mass flow of each component in the block outlet stream ELE-PYRO. The pyrolysis reactions occurred at 500 °C in PYROLYSE reactor in the presence of nitrogen environment and produced gas and oil. The streams PYRO-OUT entered the block CVD reactor. The pyrolysis product, produced from PYROLYSE, entered into the CVD, where decomposition occurred at 500, 700 and 900 °C in the presence of biochar catalyst. Carbon and hydrogen, produced from CVD process, were separated using a cyclone separator.

3. Results and discussion

3.1. Mass balance and carbon yield

Table 1 shows the carbon deposition rate (mg of carbon deposited on the surface of catalyst per g of catalyst ($mg/g_{catalyst}$)) at different temperatures and particle sizes. Carbon deposition on the surface of catalyst was estimated by the mass balance of biochar catalyst at before and after CVD experiment. Obviously, the slow pyrolysis of PPC yielded the highest gaseous products and lowest liquid products. The hydrocarbon gases, released from the PPC pyrolysis, were responsible for carbon material production in zone III at temperatures above 700 °C. These hydrocarbon gases broke down into nanostructured carbons and light gases such as CO, CO_2 or H_2. Nano carbons were found to have deposited on the surface of the biochar catalyst. It can be seen from Table 1 that the yield of carbon deposition increases with the increase in reaction temperature. The two-sample *t*-test of carbon deposition at different reaction temperatures showed a *p*-value between 0.001 and 0.011 (<0.05), which indicates the difference in carbon deposition at different reaction temperatures is statistically significant. This observation is in accordance with several previous studies, showing that the carbon deposition increases at higher temperatures (Das et al., 2006; Lee et al., 2001). The gas production increased initially with temperature due to the splitting of larger hydrocarbons into gases, which is in line with the reduction of

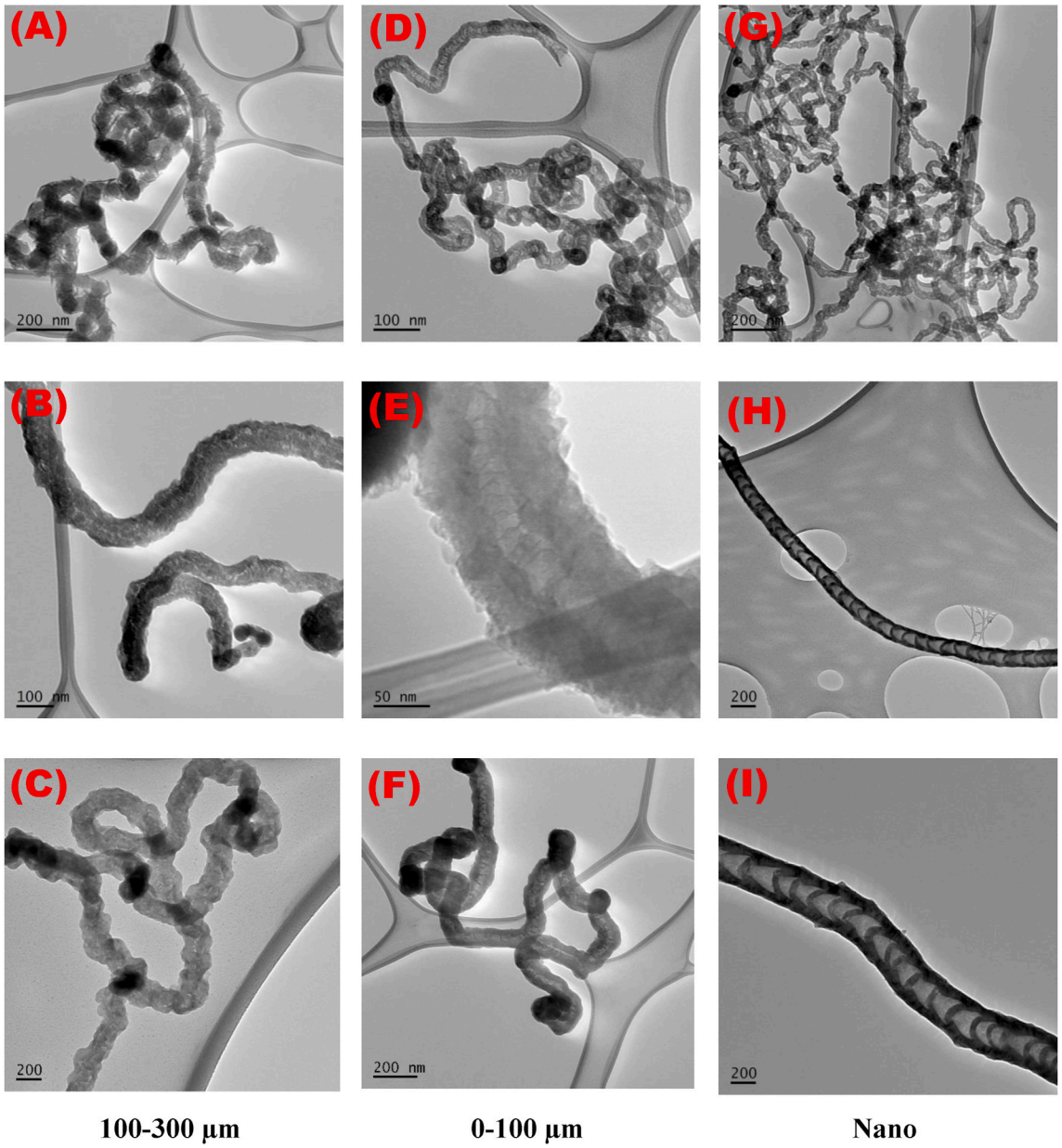

Fig. 3. TEM images of CNTs, formed at CVD temperature of 900 °C.

liquid yield. At higher temperatures, the high molecular weight components converted into low molecular weight components, and thereby, more gases transformed on the catalyst surface and converted into solid carbons through equation (1). Thus, higher solid yields were observed at higher temperatures. The carbon deposition rate was calculated as a ratio between the mass of carbon produced and the mass of the catalyst (Becker et al., 2011; Setyopratomo et al., 2018). As shown, the maximum carbon yield of 15.6 mg/$g_{catalyst}$ with gases yield of 78.15% was obtained at 900 °C in the case of nanoparticle biochar catalyst.

However, a slight difference in carbon deposition rate was noticed between 500 (1.0 mg/$g_{catalyst}$) and 700 °C (2.2 mg/$g_{catalyst}$). A similar pattern in carbon yield was also observed for µm sized particles at any specific temperature. Fig. S3 compares the modelling and experimental values of carbon deposition on the biochar surface. It was observed that experimental values of carbon deposition on the catalyst surface were much lower than those achieved from the process modelling at 900, 700 and 500 °C. This was primarily because of the variation in thermodynamic equilibrium calculations. The modelling work considered thermodynamic equilibrium calculations, whereas the experiments deviated from the equilibrium calculations. The cracking of methane on the biochar surface depends on the amount of methane transfers to the biochar surface.

$$C_xH_y \rightarrow C + H_2 \quad (1)$$

3.2. Gas product analysis

Fig. 1 illustrates the non-converted pyrolysis gas profiles in the presence of micro and nano-sized biochar particles. It can be seen from the figure that the volume of methane increases with the increase in temperature. The amount of carbon production increased, when the conversion of gases increased from higher molecular weight to lower molecular weight such as methane. The production of hydrogen was also increased with the increase of carbon deposition, as both carbon and hydrogen produced from the decomposition of hydrocarbons according

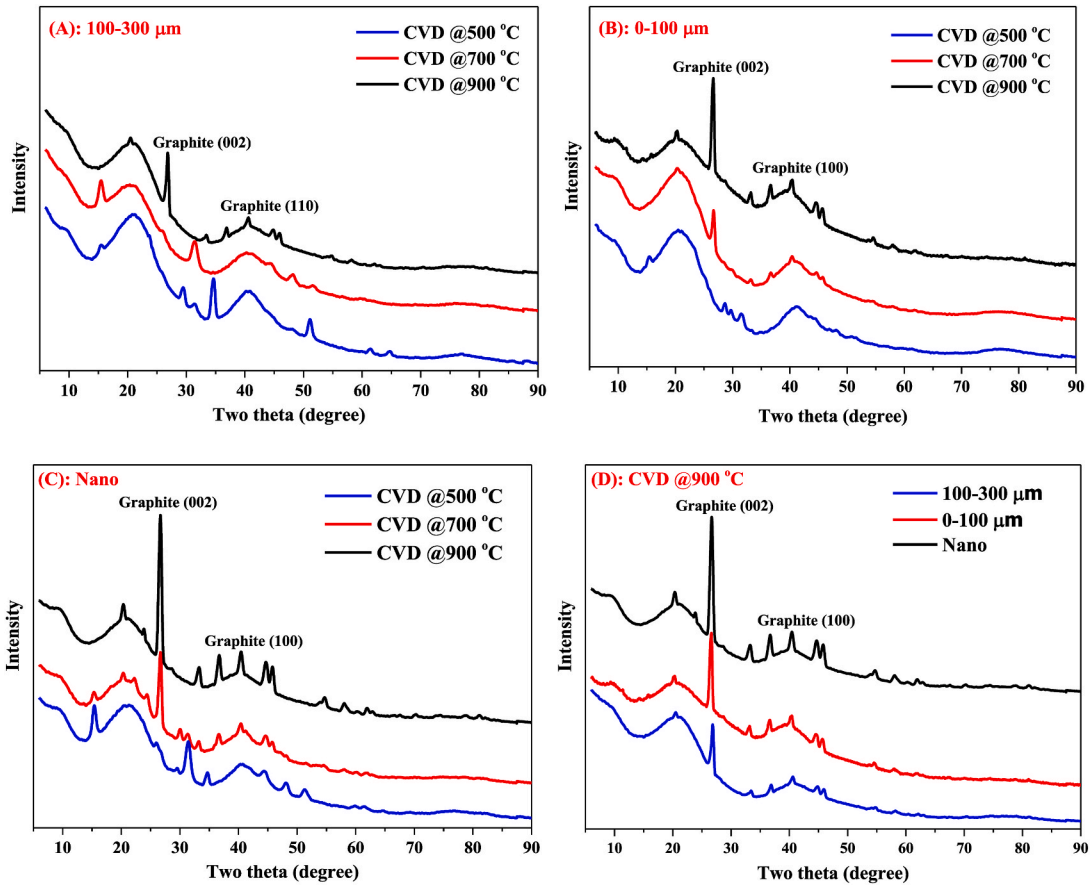

Fig. 4. XRD patterns of carbon, deposited on different biochar samples (A) 100–300 μm (B) 0–100 μm, (C) nano-sized particle and (D) at CVD temperature of 900 °C.

to Eq (1). This observation was identical with other studies on hydrogen and carbon nanotubes production (Gallego et al., 2010; Liu et al., 2011). Fig. 1 shows that the volume of C_2–C_4 gases decreases as the temperature increases since they decompose into lower molecular weight components such as methane or deposit on the catalyst in order to form solid carbon. In the presence of nano-sized biochar particles, the methane gas increased from 16 to 30 vol% and the hydrogen gas increased from 0 to 13 vol%, when the decomposition temperature increased from 500 to 900 °C. Similarly, an increasing trend of methane and hydrogen release from the reactor was also observed in the presence of 0–100 and 100–300 μm particle size. The nano-sized particles had a higher overall conversion and higher gas concentrations compared to that of μm size biochar particles.

3.3. Characterisation of solid product

3.3.1. Scanning electron microscopy

Fig. 2 shows the effect of decomposition temperature on the carbon morphology formed on the biochar surface. The carbon structure formed at 900 °C had uniform distribution (Fig. 2(G)–(I)), while at a lower temperature (700 °C) only a primary growth of CNTs was observed. However, there was no filamentous structure formation at 500 °C. Thus, the decomposition temperatures such as 500 and 700 °C are not ideal temperatures for achieving higher CNTs yield on the surface of biochar. No severe sintering or agglomeration was observed during experiments with biochar catalysts at 900 °C. The length of CNTs was very short in the case of biochar microparticles. The length and growth of CNTs on the nano-sized biochar surface was higher (Fig. 2(G)) compared to that of 0–100 and 100–300 μm particle size biochar. The biochar nanoparticles positively impacted the growth of CNTs (Esteves et al., 2018; Jourdain and Bichara, 2013; Wang et al., 2019). The strong gas-solid contact and void fraction in the case of nano-sized biochar stimulates the axial growth of CNTs (Esteves et al., 2018; Jourdain and Bichara, 2013). The nano-sized biochar catalyst produced about 30% more carbon, when compared with that of biochar with μm size particles. This was most likely due to the greater capacities of the nanoparticle catalysts during the frontal diffusion of the smaller diameters. The biochar with a larger particle size produced amorphous carbons and prohibited the formation of uniform CNTs due to the lower active site surface area with larger particle size (Liu et al., 2018c). Therefore, the process of CNTs formations can be explained by the diffusion–precipitation mechanism, which involves the diffusion of carbon to the biochar surface and carbon precipitation on the biochar. The differences in the morphology at different temperatures can be influenced by the rate of hydrocarbon decomposition to solid carbon and the diffusion rate of carbon.

3.3.2. Transmission Electron Microscopy

Fig. 3 shows TEM images of the CNTs produced on the biochar catalyst surface from the thermal decomposition of PPC waste at 900 °C at different particle sizes. The formation of concentrated CNTs was observed for every particle size, suggesting that the diffusion barrier is reduced at a higher temperature. The majority of carbon filament was made of CNTs with a central bamboo-type structure. It was seen that the growth of CNTs increased with the decrease of the particle size from 100 to 300 μm to nano-sized particle.

The variation of the biochar particle size also impacted the diameters of CNTs samples. The narrow and irregular inner hollow core were obtained at 100–300 μm size (Fig. 3(A)–(C)), which indicated the presence of many defects and rugged surface in the graphitic structure of CNTs. On the contrary, CNTs with few defects and smooth surface were observed in the case of 0–100 μm size (Fig. 3(D)–(F)), which suggested the low graphitisation degree. The nano-sized biochar produced more

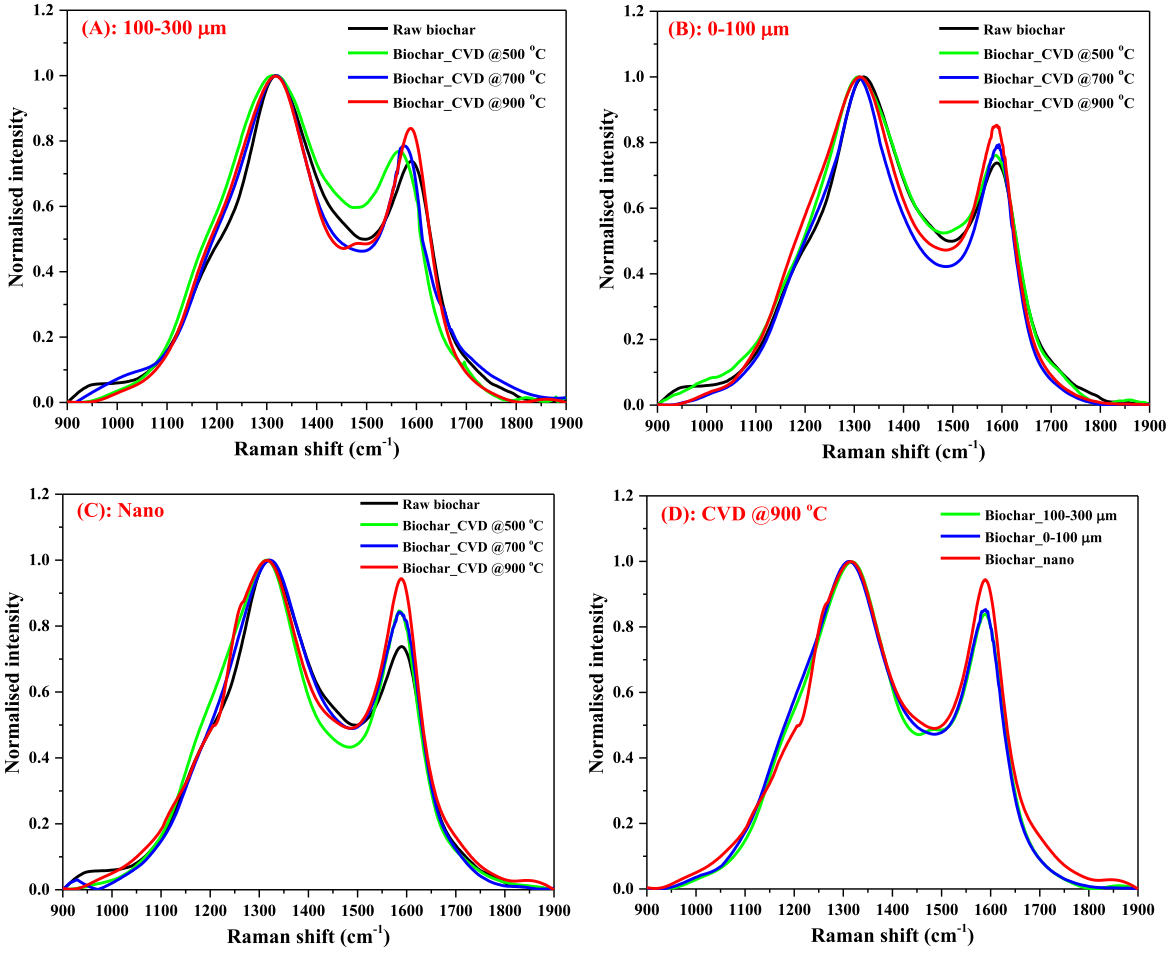

Fig. 5. Raman spectra of carbon, deposited on different biochar samples (A) 100–300 μm (B) 0–100 μm, (C) 100–300 nm and (D) at CVD temperature of 900 °C.

entangled CNTs with a diameter ranging from 50 to 100 nm (Fig. 3(G)–(I)), indicating the formation of CNTs with more uniform diameters with a complete bamboo type structure. These results prove that the uniformity and size of MWCNTs can be adjusted by varying the particle size of the catalyst.

3.3.3. XRD pattern analysis

The XRD patterns presented in Fig. 4 show the degree of graphitisation of CNTs formed on the biomass-derived biochar catalyst's surface during the CVD of oil and gas vapours produced from the pyrolysis of PPC. The peaks at angle 2Θ~26.6° and 2Θ~40.5° corresponding to the lattice plane I_{002} and I_{100} respectively represent the presence of graphite structure (Mishra et al., 2012). It can be seen from the XRD patterns that the intensity of peak at I_{002} significantly increased, when the CVD temperature was increased from 500 to 900 °C for all the biochar catalysts (Fig. 4(A)–(C)). This increase in the intensity of diffraction peak at I_{002} indicates a higher degree of graphitisation and increase in crystallinity (Chen et al., 2008). In order to investigate the effect of biochar particle size on CNTs formation, the XRD patterns of biochar samples of three different particle sizes (i.e., 100–300 μm, 0–100 μm and nano-sized particle) were compared at CVD temperature of 900 °C as shown in Fig. 4(D). An increasing trend of graphitisation was observed, when the particle size of biochar reduced from 100 to 300 μm to nano-sized particle. However, the nano-sized biochar showed the highest growth of CNTs formation with a crystallinity of 64.1% as evident in the SEM and TEM images. The interlayer spacing, also termed as d-spacing (d_{002}) values of the major graphite peak (I_{002}), were in the range of 0.334–0.335 nm, which is in agreement with the typical graphite structure (0.335 nm) (Kharisov and Kharissova, 2019). However, Ali et al. reported higher interlayer spacing value (0.349) of MWCNTs, synthesised using Ni/MgO catalyst in microwave assisted process (Ali et al., 2021).

3.3.4. Raman spectroscopic analysis

Fig. 5 shows the Raman spectra of CNTs formed on the different biochar catalysts. As can be seen from the figure, the two distinct peaks, observed at Raman shift of 1322 cm^{-1} and 1567 cm^{-1}, are termed as D and G band, respectively for all the biochar samples (Dresselhaus et al., 2005). The D band refers to the structural disorders in the graphitic layers, while the G band indicates the graphitised CNTs (Dresselhaus et al., 2002). The ratio of the intensity of G band (I_G) and D band (I_D) was used to evaluate the graphitisation degree of CNTs formed on the biochar surface. It can be seen from Fig. 5 that the value of I_G/I_D increased with the increase in CVD temperature for all the biochar samples. However, the maximum increase in I_G/I_D values (i.e., from 0.83 to 0.94) was observed in the case of nano-sized biochar samples, when the CVD temperature increased from 500 to 900 °C. The increase in I_G/I_D and I_G values at higher temperatures indicate a higher degree of graphitisation and higher quality of CNTs formation (Aboul-Enein and Awadallah, 2018). Ali et al. found a lower I_G/I_D value (0.85) of MWCNTs compared to the present study using Ni/MgO catalyst in microwave assisted process (Ali et al., 2021). However, Hidalgo et al. reported higher I_G/I_D values (0.99–1.21) of CNTs, synthesised using different agricultural wastes derived biochar and hexane via microwave assisted solvent autoignition method (Hidalgo et al., 2020). Yuan et al. also noticed a higher I_G/I_D value (1.66) of MWCNTs, produced using C_2H_4 as a carbon

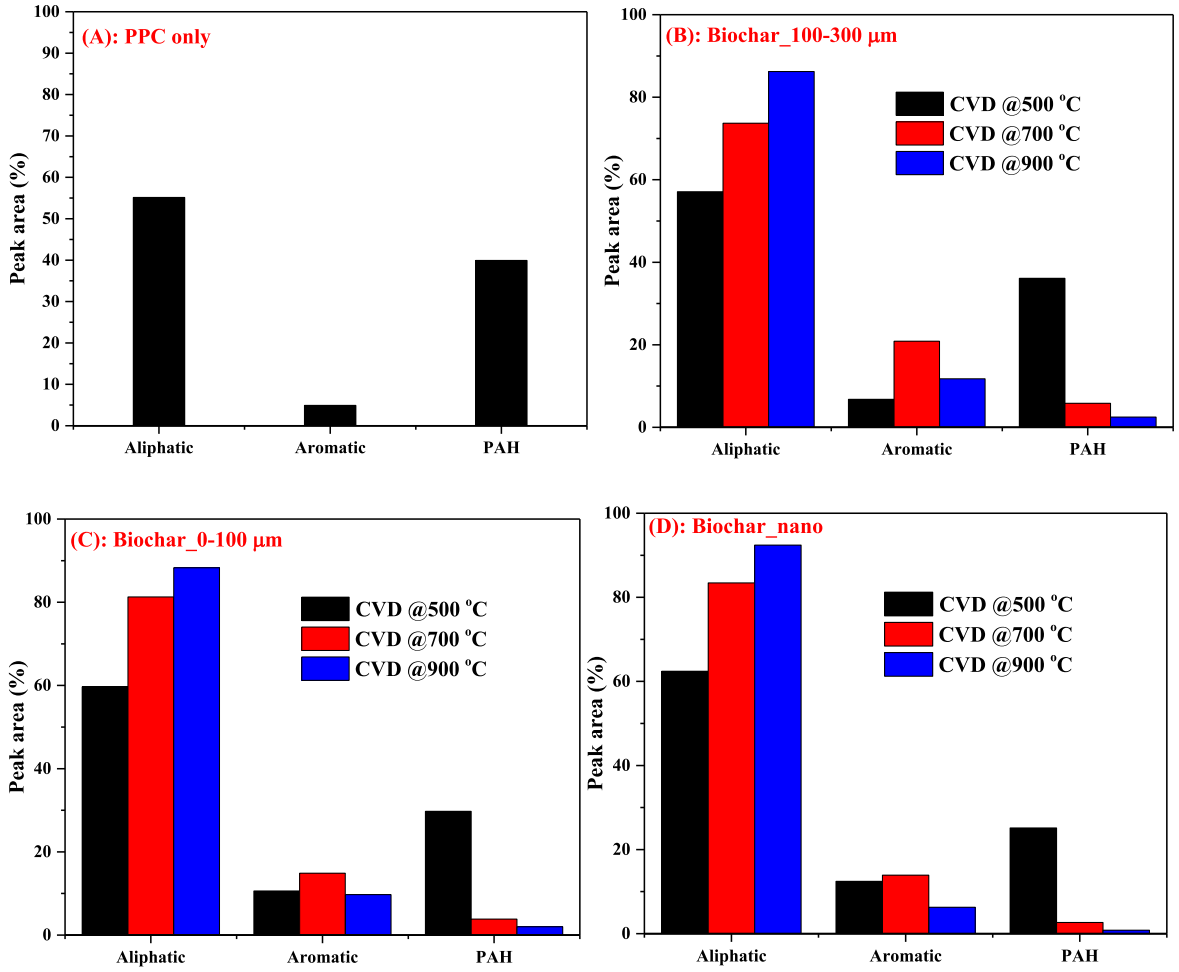

Fig. 6. Composition of oil, derived from pyrolysis of PPC only at 500 °C (A) and CVD of PPC with biochar samples of (B) 100–300 μm, (C) 0–100 μm and (D) 100–300 nm.

precursor and red soil as a catalyst in CVD process (Yuan et al., 2021). The Raman spectra of CNTs obtained using biochar of different particle sizes were compared for understanding the effect of particle size on CNTs formation as shown in Fig. 5(D). The degree of graphitisation and quality of CNTs increased with the reduction of biochar particle size; however, the nano-sized biochar sample was found to be the best in terms of quantity and quality of CNTs formation. The conclusion from the Raman spectroscopic analysis supports the findings from SEM, TEM, and XRD analysis, as discussed earlier.

3.4. Liquid product analysis

Fig. 6 shows the effect of CVD temperature and particle size of biochar catalysts on the composition of oil produced from the CVD of oil and gas vapours produced from PPC pyrolysis. The species identified in the oil was categorised into three different categories (i.e., aliphatic, aromatic and polycyclic aromatic hydrocarbons (PAH)) as depicted in Fig. 6(A)–(D). Aromatics group mainly consists of benzene and its derivatives and o-xylene, while PAHs group includes perylene, naphthalene, indene, and their derivatives. Aliphatic group is comprised of alkanes, alkenes, and their derivatives. As can be seen from Fig. 6 (A), the pyrolysis of PPC only at 500 °C produced almost 55% aliphatic, 40% PAHs, and 5% aromatic hydrocarbons. The use of biochar as a catalyst in CVD of oil and gas vapours, produced from PPC pyrolysis significantly reduced the PAH compounds. The PAH compounds are highly undesirable compounds as they are difficult to further transform and are considered to be toxic. The catalytic activity of biochar destructs the PAH compounds and enhances the formation of aliphatic and aromatic hydrocarbons, as suggested by previous literature (Patel et al., 2019) and as evident in Fig. 6. The CVD temperature significantly impacted the distribution of the oil compounds for all the biochar samples. A drastic reduction of PAH compounds (i.e., 36 to 2.5%) was observed, when the CVD temperature increased from 500 to 900 °C for biochar of particle size 100–300 μm. The nano-sized biochar sample outperformed the other biochar catalysts at CVD temperature of 900 °C with the highest aliphatic compounds (93%) formation and negligible PAH compounds (~1%) production, which is beneficial as oil with high aliphatic compounds and low PAH compounds is favourable for further utilisation.

3.5. Carbon materials from waste plastic towards circular economy and environmental sustainability

Based on the current data, approximately 80% of waste plastic undergoes incineration and landfilling, which is associated with a significant CO_2 emission and microplastic formation (Ritchie and Roser, 2020). The remaining 20% of waste plastic is recycled and used particularly for packaging, other fast-moving consumer goods and also in construction; however, majority of the current plastics recycling applications are focused on the downcycling of the plastics waste (i.e. the resulting product is of lower value than its original value). The conversion of plastics into oil can be considered upcycling. However, oil from plastics has a very high PAHs and therefore not suitable for direct use without further upgrade. Additionally, PAHs are toxic and carcinogenic, which are associated with severe human health and

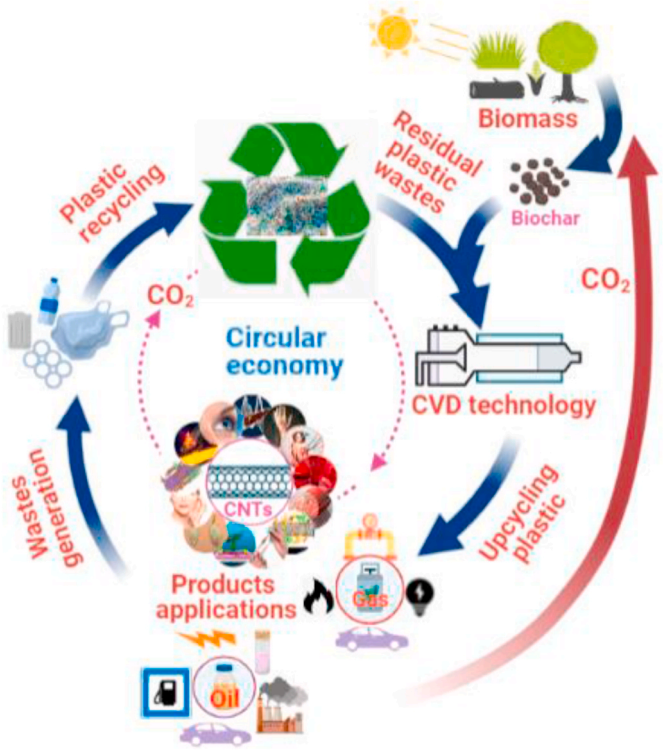

Fig. 7. Sustainable circular economy of plastic wastes via CVD process.

environmental hazards. The current study transforms plastic wastes into high-value CNTs, high-quality oil with a low PAHs and methane and hydrogen rich gas via a two-step process. Methane and hydrogen rich gas can be cleaned and used as a replacement of fossil fuel, which can provide considerable environmental benefits compared to fossil fuel, particularly when producing heat and electricity. The gas can also be used to provide energy to the pyrolysis and CVD reactions to make the overall process energy neutral. Therefore, the upcycling of plastics waste into CNTs, clean oil (with lower PAHs) and gas, as described in this study, can be certainly more appealing than currently available options and truly demonstrates an environmentally sustainable and circular economy approach. Fig. 7 shows the sustainable circular economy concept of plastic wastes via CNTs and clean oil production using biochar catalyst. Biochar, as a catalyst, offers a number of advantages. The major advantage is that it can be produced from low-cost and easily available biomass or similar wastes, which can have negative environmental impacts, when they are discarded or burnt. Production of biochar transforms carbon into a more stable form as well the CNTs synthesis process from waste plastics using biochar sequesters carbon in the form of a high-value product. Therefore, biochar can be a low-cost and sustainable catalytic material, while replacing costly metal catalysts.

4. Practical applications and future research prospects

In the past few decades, CNTs have received significant research interests due to their excellent mechanical, chemical, optical, thermal, and electrical properties (Iijima, 1991). However, large scale continuous production of CNTs is still facing a number of challenges in the area of cost-efficient designs of reactor and catalysts. The CVD process operates at extremely high temperatures and is highly endothermic in nature, requiring a significant amount of energy to sustain reaction temperature. The growth of CNTs on the catalyst surface is also limited by a number of factors such as the surface area of catalyst and the presence of functional groups (Ashik et al., 2015; Patel et al., 2019).

The current CVD reactor designs generally suffer from poor heat and mass transfer and are significantly difficult to scale-up (Moene et al., 1997). The synthetic catalysts used for CVD are also very expensive and their production may cause serious environmental pollution during the production and end of life phases. The two-stage process as proposed here integrating pyrolysis and CVD with biochar as a catalyst for plastic conversion to high-quality oil and CNTs can help minimising the negative environmental impact of catalysts as well as waste plastics. However, the challenge related to the design of CVD rector with improved heat and mass transfer still remains there. Several reactor designs such as fluidised bed, floating catalyst and inclined bed rotary systems need to be designed, developed and demonstrated for this concept. The RMIT University patented fluidised bed heat exchanger can also play an important role in demonstrating this concept at large scale (Shah, 2021). Apart from these, comprehensive mass and energy balance studies as well as techno-economic study needs to be performed for the development of scale-up rule.

Also, future research is required to identify ways of improving conversion rates as well as controlling the product quality, morphology and size of CNTs without affecting the oil quality with biochar catalyst. CNTs produced from plastic wastes using biochar catalysts should be characterised and demonstrated for a number of advanced applications in various sectors including textile, ultra-strong fibres, hydrogen storage, electronics, fuel cell, microwave absorption, manufacture of nano-cables and transistors, catalysis process, actuator and biomedical. The oil with a very low concentration of PAHs can be demonstrated for its use with minimal upgrading for energy and transport applications or for the synthesis of high-value chemicals and fuels.

The underdeveloped and developing countries are producing a huge quantity of plastic wastes, which are poorly managed due to the lack of proper management systems and awareness. Additionally, these countries have an abundant amount of biomass resources, which are usually burnt for energy purpose, leading to the environmental emission. Therefore, the current approach can be implemented in the underdeveloped and developing countries for boosting the economy of waste plastics by renewing its life as a highly priced CNT materials and oil using biomass-derived biochar catalyst.

More importantly, in the future, this process can be used to treat municipal solid waste (MSW) as shown in Fig. S4. The organic fraction of the municipal solid waste can be used to produce biochar and segregated plastics waste can be pyrolysed and passed through CVD reactor to produce CNTs and high-quality oil with biochar as catalyst. With efficient integration, the process can be a net energy generator.

5. Conclusions

Carbon nanotubes and high-quality oil were produced from waste PPC using biochar micro- and nanoparticles as catalysts in two-stage pyrolysis–catalytic reactor, which can offer an attractive circular economy. Carbon deposition was increased with the increase in reaction temperature and a larger amount of CNTs production was observed at 900 °C. This was because the growth rate of CNTs increased with reaction temperature as a result of faster carbon diffusion through the catalyst particle. This is assumed to be the rate determining step in CNT formation and the increase in diffusion leads to a larger CNT production. When compared with biochar microparticles, nano-sized biochar exhibited higher growth of CNTs formation with better quality due to their strong gas-solid contact and void fraction, which enhanced the diffusion–precipitation mechanism. Apart from these, biochar nanoparticles enhanced hydrogen production and significantly reduced polycyclic aromatic hydrocarbons in oil.

CrediT author statement

Kalpit Shah: Conceptualization, Methodology, Software, Validation, Formal analysis, Investigation, Writing - Original Draft, Writing - Review & Editing **Savankumar Patel:** Methodology, Software, Validation, Formal analysis, Investigation, Writing - Original Draft, Writing -

Review & Editing **Pobitra Halder:** Methodology, Software, Validation, Formal analysis, Investigation, Writing - Original Draft, Writing - Review & Editing **Sazal Kundu:** Formal analysis, Investigation, Writing - Original Draft, Writing - Review & Editing **Mojtaba Hedayati Marzbali:** Visualization, Writing - Review & Editing **Ibrahim Gbolahan Hakeem:** Visualization, Writing - Review & Editing **Biplob Kumar Pramanik:** Visualization, Writing - Review & Editing **Ken Chiang:** Visualization, Writing - Review & Editing **Tejas Patel:** Methodology, Investigation, Writing - Review & Editing.

Declaration of competing interest

The authors declare that they have no known competing financial interests or personal relationships that could have appeared to influence the work reported in this paper.

Acknowledgement

This work was supported by ARC DECRA Fellowship (DE170100952) and RMIT University, Melbourne, Australia.

Appendix A. Supplementary data

Supplementary data to this article can be found online at https://doi.org/10.1016/j.jenvman.2021.113791.

References

Aboul-Enein, A.A., Adel-Rahman, H., Haggar, A.M., Awadallah, A.E., 2017. Simple method for synthesis of carbon nanotubes over Ni-Mo/Al2O3 catalyst via pyrolysis of polyethylene waste using a two-stage process. Fullerenes, Nanotub. Carbon Nanostruct. 25, 211–222. https://doi.org/10.1080/1536383X.2016.1277422.

Aboul-Enein, A.A., Awadallah, A.E., 2018. A novel design for mass production of multi-walled carbon nanotubes using Co-Mo/MgO catalyst via pyrolysis of polypropylene waste: effect of operating conditions. Fullerenes, Nanotub. Carbon Nanostruct. 26, 591–605. https://doi.org/10.1080/1536383X.2018.1476344.

Aboul-Enein, A.A., Awadallah, A.E., Abdel-Rahman, A.A.-H., Haggar, A.M., 2018. Synthesis of multi-walled carbon nanotubes via pyrolysis of plastic waste using a two-stage process. Fullerenes, Nanotub. Carbon Nanostruct. 26, 443–450. https://doi.org/10.1080/1536383X.2018.1447929.

Acquavia, M.A., Pascale, R., Martelli, G., Bondoni, M., Bianco, G., 2021. Natural polymeric materials: a solution to plastic pollution from the agro-food sector. Polymers 13, 158. https://doi.org/10.3390/polym13010158.

Ahmed, W., Awadallah, A.E., Aboul-Enein, A.A., 2016. Ni/CeO2–Al2O3 catalysts for methane thermo-catalytic decomposition to COx-free H2 production. Int. J. Hydrogen Energy 41, 18484–18493. https://doi.org/10.1016/j.ijhydene.2016.08.177.

Al-Salem, S., Lettieri, P., Baeyens, J., 2009. Recycling and recovery routes of plastic solid waste (PSW): a review. Waste Manag. 29, 2625–2643. https://doi.org/10.1016/j.wasman.2009.06.004.

Ali, I., AlGarni, T.S., Burakova, E., Tkachev, A., Tugolukov, E., Dyachkova, T., Rukhov, A., Gutnik, I., Galunin, E., 2021. A new approach to the economic synthesis of multi-walled carbon nanotubes using a Ni/MgO catalyst. Mater. Chem. Phys. 261, 124234. https://doi.org/10.1016/j.matchemphys.2021.124234.

Arena, U., Mastellone, M.L., Camino, G., Boccaleri, E., 2006. An innovative process for mass production of multi-wall carbon nanotubes by means of low-cost pyrolysis of polyolefins. Polym. Degrad. Stabil. 91, 763–768. https://doi.org/10.1016/j.polymdegradstab.2005.05.029.

Ashik, U., Daud, W.W., Abbas, H.F., 2015. Production of greenhouse gas free hydrogen by thermocatalytic decomposition of methane–A review. Renew. Sustain. Energy Rev. 44, 221–256. https://doi.org/10.1016/j.rser.2014.12.025.

Awadallah, A., Aboul-Enein, A., Yonis, M., Aboul-Gheit, A., 2016. Effect of structural promoters on the catalytic performance of cobalt-based catalysts during natural gas decomposition to hydrogen and carbon nanotubes. Fullerenes, Nanotub. Carbon Nanostruct. 24, 181–189. https://doi.org/10.1080/1536383X.2015.1132206.

Bazargan, A., McKay, G., 2012. A review–synthesis of carbon nanotubes from plastic wastes. Chem. Eng. J. 195, 377–391. https://doi.org/10.1016/j.cej.2012.03.077.

Becker, M.J., Xia, W., Tessonnier, J.-P., Blume, R., Yao, L., Schlögl, R., Muhler, M., 2011. Optimizing the synthesis of cobalt-based catalysts for the selective growth of multiwalled carbon nanotubes under industrially relevant conditions. Carbon 49, 5253–5264. https://doi.org/10.1016/j.carbon.2011.07.043.

Berkmans, A.J., Jagannatham, M., Priyanka, S., Haridoss, P., 2014. Synthesis of branched, nano channeled, ultrafine and nano carbon tubes from PET wastes using the arc discharge method. Waste Manag. 34, 2139–2145. https://doi.org/10.1016/j.wasman.2014.07.004.

Biso, M., Ricci, D., 2009. Fully plastic actuator based on multi-walled carbon nanotubes bucky gel. In: 2009 9th IEEE Conference on Nanotechnology (IEEE-NANO). IEEE, pp. 481–484. https://doi.org/10.1016/j.jaap.2016.05.018.

Borsodi, N., Szentes, A., Miskolczi, N., Wu, C., Liu, X., 2016. Carbon nanotubes synthetized from gaseous products of waste polymer pyrolysis and their application. J. Anal. Appl. Pyrol. 120, 304–313. https://doi.org/10.1016/j.jaap.2016.05.018.

Chen, C.-Y., Lin, K.-Y., Tsai, W.-T., Chang, J.-K., Tseng, C.-M., 2010. Electroless deposition of Ni nanoparticles on carbon nanotubes with the aid of supercritical CO2 fluid and a synergistic hydrogen storage property of the composite. Int. J. Hydrogen Energy 35, 5490–5497. https://doi.org/10.1016/j.ijhydene.2010.03.035.

Chen, Y., Riu, D.-H., Lim, Y.-S., 2008. Carbon nanotubes grown over Fe− Mo− Mg− O composite catalysts. Met. Mater. Int. 14, 385. https://doi.org/10.3365/met.mat.2008.06.385.

Cheng, T.-C., 2012. Effect of nitrogen and hydrogen on the growth of multiwall carbon nanotubes on flexible carbon cloth using thermal chemical vapor deposition. Mater. Chem. Phys. 136, 140–145. https://doi.org/10.1016/j.matchemphys.2012.06.043.

Chhowalla, M., Teo, K., Ducati, C., Rupesinghe, N., Amaratunga, G., Ferrari, A., Roy, D., Robertson, J., Milne, W., 2001. Growth process conditions of vertically aligned carbon nanotubes using plasma enhanced chemical vapor deposition. J. Appl. Phys. 90, 5308–5317. https://doi.org/10.1063/1.1410322.

Chung, Y.-H., Jou, S., 2005. Carbon nanotubes from catalytic pyrolysis of polypropylene. Mater. Chem. Phys. 92, 256–259. https://doi.org/10.1016/j.matchemphys.2005.01.023.

Das, N., Dalai, A., Mohammadzadeh, J.S.S., Adjaye, J., 2006. The effect of feedstock and process conditions on the synthesis of high purity CNTs from aromatic hydrocarbons. Carbon 44, 2236–2245. https://doi.org/10.1016/j.carbon.2006.02.040.

Dresselhaus, M., Dresselhaus, G., Jorio, A., Souza Filho, A., Saito, R., 2002. Raman spectroscopy on isolated single wall carbon nanotubes. Carbon 40, 2043–2061. https://doi.org/10.1016/S0008-6223(02)00066-0.

Dresselhaus, M.S., Dresselhaus, G., Saito, R., Jorio, A., 2005. Raman spectroscopy of carbon nanotubes. Phys. Rep. 409, 47–99. https://doi.org/10.1016/j.physrep.2004.10.006.

Esteves, L.M., Oliveira, H.A., Passos, F.B., 2018. Carbon nanotubes as catalyst support in chemical vapor deposition reaction: a review. J. Ind. Eng. Chem. 65, 1–12. https://doi.org/10.1016/j.jiec.2018.04.012.

Gallego, G.S., Barrault, J., Batiot-Dupeyrat, C., Mondragón, F., 2010. Production of hydrogen and MWCNTs by methane decomposition over catalysts originated from LaNiO3 perovskite. Catal. Today 149, 365–371. https://doi.org/10.1016/j.cattod.2009.06.004.

Ghosh, S.K., 2018. Waste Management and Resource Efficiency: Proceedings of 6th IconSWM 2016. Springer. https://doi.org/10.1007/978-981-10-7290-1.

Gong, J., Liu, J., Jiang, Z., Feng, J., Chen, X., Wang, L., Mijowska, E., Wen, X., Tang, T., 2014. Striking influence of chain structure of polyethylene on the formation of cup-stacked carbon nanotubes/carbon nanofibers under the combined catalysis of CuBr and NiO. Appl. Catal. B Environ. 147, 592–601. https://doi.org/10.1016/j.apcatb.2013.09.044.

Gong, J., Liu, J., Wan, D., Chen, X., Wen, X., Mijowska, E., Jiang, Z., Wang, Y., Tang, T., 2012. Catalytic carbonization of polypropylene by the combined catalysis of activated carbon with Ni2O3 into carbon nanotubes and its mechanism. Appl. Catal. Gen. 449, 112–120. https://doi.org/10.1016/j.apcata.2012.09.028.

Gong, J., Yao, K., Liu, J., Wen, X., Chen, X., Jiang, Z., Mijowska, E., Tang, T., 2013. Catalytic conversion of linear low density polyethylene into carbon nanomaterials under the combined catalysis of Ni2O3 and poly (vinyl chloride). Chem. Eng. J. 215, 339–347. https://doi.org/10.1016/j.cej.2012.11.037.

Guerrero, A., Puerta, J., Gomez, F., Blanco, F., 2008. Synthesis of carbon nanotubes by laser ablation in graphite substrate of industrial arc electrodes. Phys. Scripta 2008, 014007. https://doi.org/10.1088/0031-8949/2008/T131/014007.

Hidalgo, P., Coronado, G., Sánchez, A., Hunter, R., 2020. Agro-industrial waste as precursor source for carbon nanotubes (CNTs) synthesis using a new technical of solvent autoignition. In: IOP Conference Series: Earth and Environmental Science. IOP Publishing. https://doi.org/10.1016/j.jenvman.2019.03.082, 012025.

Hildago-Oporto, P., Navia, R., Hunter, R., Coronado, G., Gonzalez, M., 2019. Synthesis of carbon nanotubes using biochar as precursor material under microwave irradiation. J. Environ. Manag. 244, 83–91. https://doi.org/10.1016/j.jenvman.2019.03.082.

Iijima, S., 1991. Helical microtubules of graphitic carbon. Nature 354, 56–58. https://doi.org/10.1038/354056a0.

In, J.B., Grigoropoulos, C.P., Chernov, A.A., Noy, A., 2011. Growth kinetics of vertically aligned carbon nanotube arrays in clean oxygen-free conditions. ACS Nano 5, 9602–9610. https://doi.org/10.1021/nn2028715.

Jin, G.-P., Ding, Y.-F., Zheng, P.-P., 2007. Electrodeposition of nickel nanoparticles on functional MWCNT surfaces for ethanol oxidation. J. Power Sources 166, 80–86. https://doi.org/10.1016/j.jpowsour.2006.12.087.

Jourdain, V., Bichara, C., 2013. Current understanding of the growth of carbon nanotubes in catalytic chemical vapour deposition. Carbon 58, 2–39. https://doi.org/10.1016/j.carbon.2013.02.046.

Kalita, G., Adhikari, S., Aryal, H.R., Afre, R., Soga, T., Sharon, M., Umeno, M., 2009. Functionalization of multi-walled carbon nanotubes (MWCNTs) with nitrogen plasma for photovoltaic device application. Curr. Appl. Phys. 9, 346–351. https://doi.org/10.1016/j.cap.2008.03.007.

Kang, T.J., Choi, A., Kim, D.-H., Jin, K., Seo, D.K., Jeong, D.H., Hong, S.-H., Park, Y.W., Kim, Y.H., 2010. Electromechanical properties of CNT-coated cotton yarn for electronic textile applications. Smart Mater. Struct. 20, 015004 https://doi.org/10.1088/0964-1726/20/1/015004.

Kharisov, B.I., Kharissova, O.V., 2019. Carbon Allotropes: Metal-Complex Chemistry, Properties and Applications. Springer. https://doi.org/10.1007/978-3-030-03505-1.

Kong, Q., Zhang, J., 2007. Synthesis of straight and helical carbon nanotubes from catalytic pyrolysis of polyethylene. Polym. Degrad. Stabil. 92, 2005–2010. https://doi.org/10.1016/j.polymdegradstab.2007.08.002.

Lee, C.J., Park, J., Huh, Y., Lee, J.Y., 2001. Temperature effect on the growth of carbon nanotubes using thermal chemical vapor deposition. Chem. Phys. Lett. 343, 33–38. https://doi.org/10.1016/S0009-2614(01)00680-7.

Lefebvre, J., Ding, J., 2017. Carbon nanotube thin film transistors by droplet electrophoresis. Materials Today Communications 10, 72–79. https://doi.org/10.1016/j.mtcomm.2017.01.002.

Liu, B., Lee, T., Lee, S., Park, C., Lee, C.J., 2003. Large-scale synthesis of high-purity well-aligned carbon nanotubes using pyrolysis of iron (II) phthalocyanine and acetylene. Chem. Phys. Lett. 377, 55–59. https://doi.org/10.1016/S0009-2614(03)01092-3.

Liu, G., Zheng, H., Jiang, Z., Zhao, J., Wang, Z., Pan, B., Xing, B., 2018a. Formation and physicochemical characteristics of nano biochar: insight into chemical and colloidal stability. Environ. Sci. Technol. 52, 10369–10379. https://doi.org/10.1021/acs.est.8b01481.

Liu, J., Jiang, Z., Yu, H., Tang, T., 2011. Catalytic pyrolysis of polypropylene to synthesize carbon nanotubes and hydrogen through a two-stage process. Polym. Degrad. Stabil. 96, 1711–1719. https://doi.org/10.1016/j.polymdegradstab.2011.08.008.

Liu, L., Lou, H., Chen, M., 2018b. Selective hydrogenation of furfural over Pt based and Pd based bimetallic catalysts supported on modified multiwalled carbon nanotubes (MWNT). Appl. Catal. Gen. 550, 1–10. https://doi.org/10.1016/j.apcata.2017.10.003.

Liu, X., Shen, B., Wu, Z., Parlett, C.M., Han, Z., George, A., Yuan, P., Patel, D., Wu, C., 2018c. Producing carbon nanotubes from thermochemical conversion of waste plastics using Ni/ceramic based catalyst. Chem. Eng. Sci. 192, 882–891. https://doi.org/10.1016/j.ces.2018.07.047.

Louisia, S., Contreras, R.C., Heitzmann, M., Axet, M.R., Jacques, P.-A., Serp, P., 2018. Sequential catalytic growth of sulfur-doped carbon nanotubes and their use as catalyst support. Catal. Commun. 109, 65–70. https://doi.org/10.1016/j.catcom.2018.02.024.

Mishra, N., Das, G., Ansaldo, A., Genovese, A., Malerba, M., Povia, M., Ricci, D., Di Fabrizio, E., Di Zitti, E., Sharon, M., 2012. Pyrolysis of waste polypropylene for the synthesis of carbon nanotubes. J. Anal. Appl. Pyrol. 94, 91–98. https://doi.org/10.1016/j.jaap.2011.11.012.

Moene, R., Tazelaar, F., Makkee, M., Moulijn, J., 1997. Nickel-catalyzed conversion of activated carbon extrudates into high surface area silicon carbide by reactive chemical vapour deposition. J. Catal. 170, 311–324. https://doi.org/10.1006/jcat.1997.1782.

Nahil, M.A., Wu, C., Williams, P.T., 2015. Influence of metal addition to Ni-based catalysts for the co-production of carbon nanotubes and hydrogen from the thermal processing of waste polypropylene. Fuel Process. Technol. 130, 46–53. https://doi.org/10.1016/j.fuproc.2014.09.022.

Narayanan, T., Sunny, V., Shaijumon, M., Ajayan, P., Anantharaman, M., 2009. Enhanced microwave absorption in nickel-filled multiwall carbon nanotubes in the S band. Electrochem. Solid State Lett. 12, K21–K24. https://doi.org/10.1149/1.3065992.

Paradise, M., Goswami, T., 2007. Carbon nanotubes–production and industrial applications. Mater. Des. 28, 1477–1489. https://doi.org/10.1016/j.matdes.2006.03.008.

Patel, S., Kundu, S., Halder, P., Veluswamy, G., Pramanik, B., Paz-Ferreiro, J., Surapaneni, A., Shah, K., 2019. Slow pyrolysis of biosolids in a bubbling fluidised bed reactor using biochar, activated char and lime. J. Anal. Appl. Pyrol. 144, 104697. https://doi.org/10.1016/j.jaap.2019.104697.

Perez-Cabero, M., Rodrıguez-Ramos, I., Guerrero-Ruız, A., 2003. Characterization of carbon nanotubes and carbon nanofibers prepared by catalytic decomposition of acetylene in a fluidized bed reactor. J. Catal. 215, 305–316. https://doi.org/10.1016/S0021-9517(03)00026-5.

Qin, Y., Zhang, Q., Cui, Z., 2004. Effect of synthesis method of nanocopper catalysts on the morphologies of carbon nanofibers prepared by catalytic decomposition of acetylene. J. Catal. 223, 389–394. https://doi.org/10.1016/j.jcat.2004.02.004.

Reddy, N.K., Meunier, J.-L., Coulombe, S., 2006. Growth of carbon nanotubes directly on a nickel surface by thermal CVD. Mater. Lett. 60, 3761–3765. https://doi.org/10.1016/j.matlet.2006.03.109.

Ren, F., Kanaan, S.A., Majewska, M.M., Keskar, G.D., Azoz, S., Wang, H., Wang, X., Haller, G.L., Chen, Y., Pfefferle, L.D., 2014. Increase in the yield of (and selective synthesis of large-diameter) single-walled carbon nanotubes through water-assisted ethanol pyrolysis. J. Catal. 309, 419–427. https://doi.org/10.1016/j.jcat.2013.10.007.

Ritchie, H., Roser, M., 2020. Plastic Pollution. Our World in Data. Accessed on. https://ourworldindata.org/plastic-pollution. (Accessed 11 November 2020).

Savva, P.G., Polychronopoulou, K., Ryzkov, V., Efstathiou, A.M., 2010. Low-temperature catalytic decomposition of ethylene into H2 and secondary carbon nanotubes over Ni/CNTs. Appl. Catal. B Environ. 93, 314–324. https://doi.org/10.1016/j.apcatb.2009.10.005.

Setyopratomo, P., Wulan, P., Sudibandriyo, M., 2018. The effect of metal loading on the performance of tri-metallic supported catalyst for carbon nanotubes synthesis from liquefied petroleum gas. Int. J. Technolo 9, 120. https://doi.org/10.14716/ijtech.v9i1.1165.

Shah, K., 2021. A pyrolysis reaction system and method of pyrolysing an organic feed. U. S. Patent Application 17/058,760, filed July 8, 2021. (US20210207033A1).

Shaikjee, A., Coville, N.J., 2012. The role of the hydrocarbon source on the growth of carbon materials. Carbon 50, 3376–3398. https://doi.org/10.1016/j.carbon.2012.03.024.

Shirazi, Y., Tofighy, M.A., Mohammadi, T., Pak, A., 2011. Effects of different carbon precursors on synthesis of multiwall carbon nanotubes: purification and Functionalization. Appl. Surf. Sci. 257, 7359–7367. https://doi.org/10.1016/j.apsusc.2011.03.146.

Song, R., Ji, Q., 2011. Synthesis of carbon nanotubes from polypropylene in the presence of Ni/Mo/MgO catalysts via combustion. Chem. Lett. 40, 1110–1112. https://doi.org/10.1246/cl.2011.1110.

Wang, J., Shen, B., Lan, M., Kang, D., Wu, C., 2019. Carbon nanotubes (CNTs) production from catalytic pyrolysis of waste plastics: the influence of catalyst and reaction pressure. Catal. Today. https://doi.org/10.1016/j.cattod.2019.01.058.

Yuan, X., Liang, C., Ruan, C., Chang, Y., Xu, L., Huang, H., Chen, M., Yong, Z., 2021. Low-cost synthesis of multi-walled carbon nanotubes using red soil as catalyst. Diam. Relat. Mater. 112, 108241. https://doi.org/10.1016/j.diamond.2021.108241.

Zanello, L.P., Zhao, B., Hu, H., Haddon, R.C., 2006. Bone cell proliferation on carbon nanotubes. Nano Lett. 6, 562–567. https://doi.org/10.1021/nl051861e.

Zhang, J., Li, J., Cao, J., Qian, Y., 2008. Synthesis and characterization of larger diameter carbon nanotubes from catalytic pyrolysis of polypropylene. Mater. Lett. 62, 1839–1842. https://doi.org/10.1016/j.matlet.2007.10.015.

Zhang, J., Tahmasebi, A., Omoriyekomwan, J.E., Yu, J., 2019. Production of carbon nanotubes on bio-char at low temperature via microwave-assisted CVD using Ni catalyst. Diam. Relat. Mater. 91, 98–106. https://doi.org/10.1016/j.diamond.2018.11.012.

Zhuo, C., Alves, J.O., Tenorio, J.A., Levendis, Y.A., 2012. Synthesis of carbon nanomaterials through up-cycling agricultural and municipal solid wastes. Ind. Eng. Chem. Res. 51, 2922–2930. https://doi.org/10.1021/ie202711h.

Zhuo, C., Levendis, Y.A., 2014. Upcycling waste plastics into carbon nanomaterials: a review. J. Appl. Polym. Sci. 131 https://doi.org/10.1002/app.39931.